

Depth dose enhancement in the presence of silicone gel breast prosthesis

M.E. Sithole*

Department of Physics, Sefako Makgatho Health Sciences University, South Africa

ABSTRACT

Background: External beam radiation therapy is often administered to patients implanted with silicone gel breast prosthesis. The aim of this study was to investigate the influence of silicone gel breast prosthesis on photon dose distributions. In the event of recurrence, the oncologist may be forced to irradiate through the prosthetic device. To quantify the dose enhancement or reduction below the silicone gel breast prosthesis, depth dose enhancement factors (DEFs) were calculated. **Materials and Methods:** The study was based on Varian linear accelerator (LINAC) operated at 6 and 15 MV photon energies. Monte Carlo package Electron Gamma Shower (EGSnrc) was employed to simulate the depth dose distribution in a three dimensional scanning water phantom with various field sizes. The polydimethyl silicone gel breast prosthesis with density of 0.97 g/cm^3 was used. The measured and calculated DEFs were verified by using the thermoluminescent dosimeter (TLD). **Results:** The results indicate that the percentage difference between the calculated and measured dose distributions on depth dose curves for 6 and 15 photon energies was less than 2% for all locations. DEFs at 0.5 cm below the 3.5 cm prosthesis were 0.99 and 1.02 for 6 and 15 MV photon beams, respectively. The interface region receives enhanced dose of about 2.4% with 15 MV photon beam while the 6 MV photon beam delivered a dose reduction of about 2.0%. **Conclusion:** It was observed that DEFs increase with photon beam energy. The 6 MV photon beam reduces dose enhancement factor compared to that of the 15 MV photon beam.

Keywords: Dose calculation, dose enhancement factor, Monte Carlo, Silicone gel breast prosthesis, photon beam.

INTRODUCTION

When a photon beam passes through one medium to another having a different atomic number (Z), the equilibrium of charged particle is disturbed at that interface. A region exists within the interface which is composed of electron fluence generated in both media⁽¹⁾. The region may extend to a few millimeters depending on the energy of the photon beam⁽²⁾. The effect of radiation through an interface region has long been a subject of investigation⁽³⁻⁹⁾. Several authors have quantitatively calculated or measured the effect of prostheses on dose distributions^(10, 14). A study by

Roberts (2001) recommended that passing the radiation beam through a prosthetic device before reaching a target volume should be avoided⁽¹⁵⁾. However, this is not always possible in cases such as silicone gel breast prosthesis. Breast reconstruction is a type of surgery for women who have had a breast removed (mastectomy)⁽¹⁶⁾.

Dose distributions in and under the silicone gel breast prosthesis were studied during irradiation with 60Co and 4 MV photon beams⁽¹⁷⁾. The percentage errors in experimental values compared with calculated values were found to be within 2.8%. The effect of silicone gel breast prosthesis on the absorbed dose

distribution of 9-20 MeV electron beams and 1.25-15 MV photon beams was studied (18). At the depths beyond the therapeutic range, the electron beams appear to be more penetrating due to the presence of prosthesis. The dose differences were observed to vary from 0.5% to 4.0% of the maximum dose in water. The changes in the photon dose distributions due to the breast prosthesis were also measured (19). A 6 MV photon beam defined at $10 \times 10 \text{ cm}^2$ field size with a 45° wedge was used. Their results showed no significant alteration of depth doses 5 cm away from the prosthesis with minor interface perturbations for all their implants.

Based on the known principles of interaction of radiation with human tissue, the transport of energy into the patient's body can be modeled and calculated using Monte Carlo simulation (20). If the modeling has been successfully done, exact results of the dose distributions can be calculated. The increase of the number of electrons in the beam is expected because the spatial distribution of absorbed dose in a medium near an interface is a function of their relative atomic numbers and the direction of the photon beam. For a photon beam travelling from a material with a high atomic number to a material with a lower atomic number the equilibrium fluence is higher in the former because of the production of more electrons by lower energy scattering photons (21).

The aim of radiotherapy is to maximize the dose applied to the tumour below the silicone gel breast prosthesis while keeping the dose to the surrounding tissue as low as possible. The aim of this study is to investigate the influence of the silicone gel breast prosthesis on dose distribution in water phantom. Calculations using Monte Carlo method was performed in region directly below (distal region) the prosthesis. We define the dose enhancement factor as the ratio of the dose at a depth with the prosthesis in place to the dose at the same depth in water without the prosthesis. Thus a dose enhancement is obtained if $\text{DEF} > 1.0$, while a dose reduction is observed if $\text{DEF} < 1.0$. Under the same conditions as the MC simulations, the thermoluminescent dosimeter was used to

measure dose distributions to verify the validity of the Monte Carlo results. TLDs have been used in quality assurance protocols in radiotherapy (22).

MATERIALS AND METHODS

We explored the dose enhancement when photon beam is passing through the silicone gel breast prosthesis in water. Water is always assumed to be a good phantom for being close to human body (23).

Monte Carlo simulation

The study was based on a model of the 2100 C Varian linear accelerator (Varian Oncology systems, Palo Alto, California) head operated at nominal photon energies of 6 and 15 MV. The Monte Carlo code employed in this work is the EGSnrc Version 3 (24,25). The accelerator head components were simulated by using BEAMnrc user-code (26-28) and the dose in water phantom was calculated using DOSXYZnrc user-code (29). The parameters used during simulations were $\text{AE} = \text{ECUT} = 0.7 \text{ MeV}$ and $\text{AP} = \text{PCUT} = 0.01 \text{ MeV}$, where AE and AP are the electron and photon low energy thresholds for the production of secondary Bremsstrahlung photons while ECUT and PCUT are the global cutoff energy for electron and photon transport, respectively. The geometrical input data for the 6 and 15 MV photon beams were based on specifications provided by the manufacturer (30). The geometry and the material used during simulation reflected a realistic construction of the linear accelerator. The squared fields with side lengths of 5, 10, 15 and 20 cm were defined at source-surface distance (SSD) of 100 cm.

Linear accelerator head model

The user code BEAMnrc was used to simulate photon beams. The code uses a series of component modules (CMs) to model each component of a LINAC head. The target, primary collimator, flattening filter, monitor chamber, mirror and secondary collimator were constructed using the following component

modules SLAB, CONS3R, FLATFILT, CHAMBER, MIRROR AND DYNJAWS, respectively. DYNJAWS has been incorporated in the BEAMnrc code for modelling the enhanced dynamic wedge.

This code is capable of simulating an enhanced dynamic wedge using the step and shoot and dynamic delivery techniques. The phase space file obtained as BEAMnrc output was used as the input data for the calculations in water phantom⁽³¹⁾. The origin of the coordinate system $(x, y, z) = (0, 0, 0)$ was located at the front surface of the target where the electrons are incident. The isocenter of the model was defined at $(x, y, z) = (0, 0, 100)$ cm.

Phantom calculation

Silicone gel breast prosthesis used in this study consists of polydimethyl $[(\text{CH}_3)_2\text{SiO}]_n$ with physical density of 0.97 g/cm³ and the effective atomic number of 10.37⁽³²⁾. Silicone gel breast prosthesis is characterized by a thin silicone containing transparent gel which is soft⁽³³⁾. In this study six silicone gel breast prostheses of different thicknesses were used. In most calculations, a standard 400 cc silicone gel breast prosthesis with typical dimensions of 14.5 cm width and 3.5 cm thick was used. In all setups, the surface of the prosthesis was aligned to the surface of the water as shown in figure 1. The materials used to construct a water phantom were chosen from PEGS4 cross sectional data file. The medium of the region surrounding the phantom was chosen to be a vacuum. Figure 1 shows the schematic diagram of an inhomogeneous phantom designed to facilitate the position of silicone gel breast prosthesis as well as TLDs at various levels.

Calculations using TLDs were performed along the central plane of the beam under similar conditions as during measurements. The TLDs were placed below the prosthesis in water phantom as shown in figure 1. Aluminium oxide (Al_2O_3) and lithium fluoride (LiF) dosimeters were each modelled as a square chip with dimensions of $0.1 \times 0.1 \times 0.1$ cm³. The mass densities of Al_2O_3 and LiF were set to 3.97 and 2.64 g cm⁻³, respectively. The composition of the Al_2O_3 dosimeter by relative weight was O: 0.4708 and Al: 0.5292^(34, 35) while for LiF was Li: 0.6138 and F: 0.3862^(36, 37).

Measurements

Monoenergetic gamma beam cesium (Cs-137) was used to calibrate the TLDs. All TLDs were exposed under a dose of 1 mGy. 24 hours later the TLDs were read and annealed. The readout in calibration was given a correction factor of 1.5. The thermoluminescent (TL) responses of each TLD were recorded under 200 monitor units (MU) of irradiation with a 10×10 cm² field size. This step was repeated three times for each depth. The response of the whole batch was normalized to the average of all TLDs in the batch. TLDs were calibrated using the ion chamber. Measurements conducted in water phantom were carried out using a 0.6 cc ion chamber (PTW, Freiburg, Germany) for dose distribution under the same conditions. A three dimensional scanning water phantom system (RFA-300, Scanditronix, Wellhofer, Germany) was used to scan depth doses. For each field size and depth, the procedure for central percentage depth dose measurement was repeated three times.

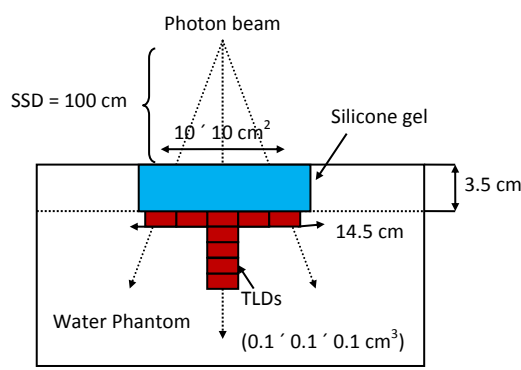


Figure 1. Inhomogeneous phantom.

RESULTS

Verification of the Monte Carlo model

MC results were compared with the experimental results conducted under similar conditions. Comparison has proven to replicate data within 2%. Maximum values of gamma index (γ) for $10 \times 10 \text{ cm}^2$ field size at the maximum dose (d_{\max}) were 0.78 and 0.63 for 6 and 15 MV photon beams, respectively. Similar results were obtained by Krishman *et al.* (1983) (38). The statistical uncertainties in MC calculations were less than 1.0%. This indicates that the calculated data has passed the acceptance test (39). The discrepancy observed at a given depth beyond the d_{\max} between the calculated and measured doses for both photon beams was within 2%. This shows an overall statistical tightness in the data.

Depth dose profiles

Depth dose distributions were calculated and analyzed as a function of depth in water with and without the silicone gel breast prosthesis in place. Figure 2 presents the depth dose curves for the 6 and 15 MV photon beams with $10 \times 10 \text{ cm}^2$ field size defined at SSD of 100 cm. The central depth dose distributions with and without the silicone gel breast prosthesis were compared. The difference between the two values at each depth was expressed as the percentage difference of the dose in water. The close agreement of MC results can be observed.

DEF on Silicone gel breast prosthesis thickness

Table 1 gives the comparison data between the measured and calculated DEFs at 0.5 cm depth below the silicone gel breast prosthesis. The proportion of DEFs in all thickness was observed to increase with the photon beam energy. The measured dose enhancement factors were observed to be higher than those obtained from the MC calculation. This is due to the large portion of high energy as well as low energy photons in the output of the MC

simulations. The dose enhancement factor decreased from 1.8% to 1.2% as the thickness was increased from 2.3 cm to 4.1 cm. By increasing the silicone gel thickness by 0.3 cm, the dose enhancement factor was increased by 0.1%. It can be seen that dose enhancement factors increase generally with photon beam energy. This is due to secondary electron fluence, which increases with photon energy.

Dependence of DEF on silicone gel thickness

Figures 3 and 4 show the dose enhancement factors for 6 and 15 MV photon beams calculated as a function of silicone gel breast thicknesses, respectively. Ten silicone gel breast prostheses with thickness ranging from 2.1 cm to 4.1 cm were used. The same silicone gel breast prosthesis placed in a water phantom was irradiated at different times with 6 and 15 MV photon beams.

Validation of the simulated DEFs

To evaluate the validity of the calculated DEFs, the TLDs were placed at the depth of 0.5 cm in a water phantom below the silicone gel breast prosthesis. Table 2 gives the comparison data for DEFs calculated and measured with TLDs. The DEFs were calculated in the voxels filled with LiF and Al_2O_3 . The measured data was acquired with LiF and Al_2O_3 chips placed at the same depth in a water phantom. The uncertainty for TLDs used during measurements was less than 2%.

The TLDs were read 24 hours later after the phantom was exposed to both beams. The readouts were converted into dose by linear interpolation based on the TLDs dose response curve. The average values obtained at 0.5 cm depth below the silicone gel breast prosthesis are shown in table 2. Besides the different material used, the DEFs were compared and found to be within 1.0%. Measurements obtained with both the TLD materials showed higher results as compared with the calculated data, especially the Al_2O_3 which is about 17% higher than the DEF values measured in water.

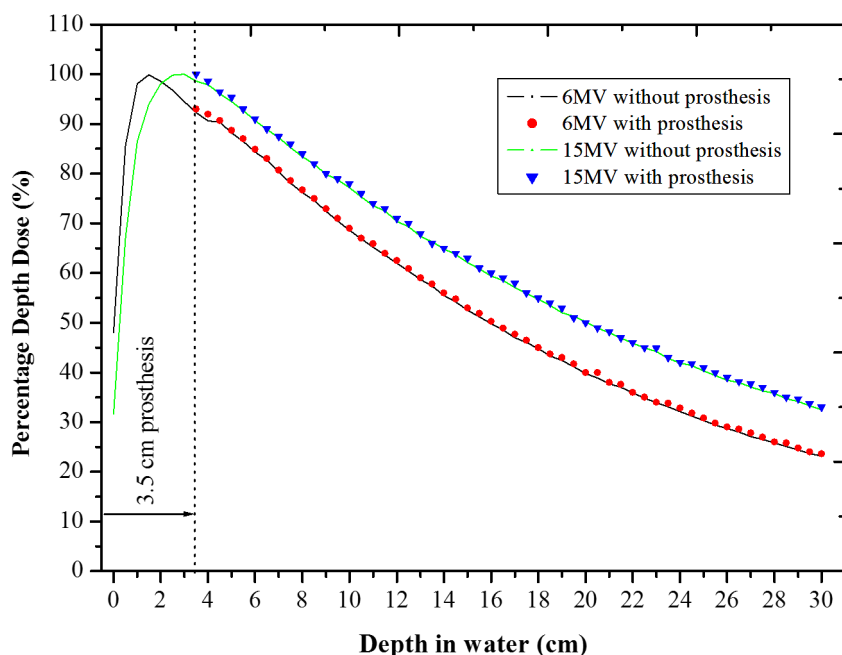


Figure 2. Percentage depth dose distribution curves for $10 \times 10 \text{ cm}^2$ field size, calculated with and without the silicone gel breast prosthesis for 6 and 15 MV photon beams.

Table 1. DEFs at 0.5 cm depth below the silicone gel breast prosthesis.

Thickness (cm)	6 MV			15 MV			
	Thickness (cm)	Mea	Cal	% Dif	Mea	Cal	% Dif
2.3	0.998	0.993		0.5	1.012	1.010	0.2
2.6	0.995	0.992		0.3	1.010	1.009	0.1
3.1	0.993	0.991		0.2	1.009	1.008	0.1
3.5	0.992	0.990		0.2	1.008	1.006	0.2
3.8	0.989	0.988		0.1	1.006	1.005	0.1
4.1	0.986	0.984		0.2	1.004	1.004	0.0

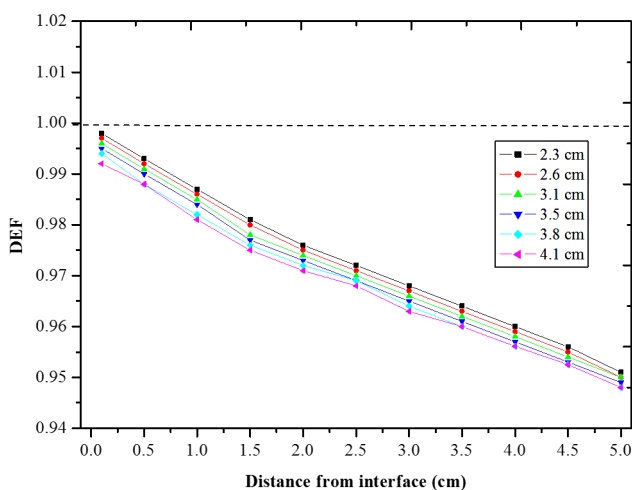


Figure 3. Dose enhancement factor for varies silicone gel thickness as a function of distance for the 6 MV photon beam with $10 \times 10 \text{ cm}^2$ field size.

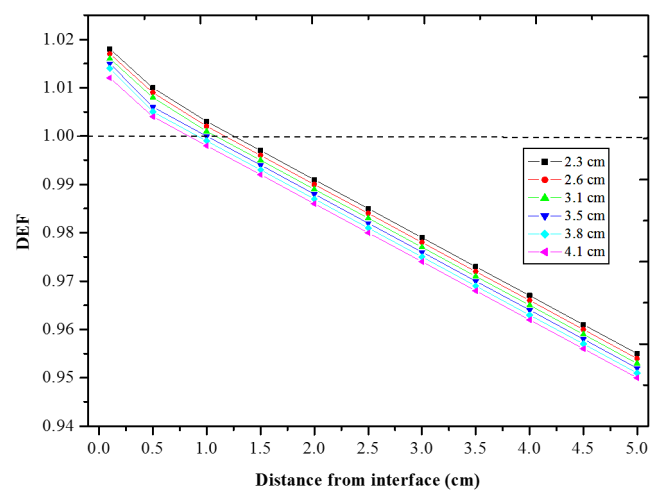


Figure 4. Dose enhancement factor for varies silicone gel thickness as a function of distance from the interface for the 15 MV photon beam with $10 \times 10 \text{ cm}^2$ field size.

Table 2. DEFs at 0.5 cm below the 3.5 cm silicone gel breast prosthesis.

	6 MV			15 MV		
	Mea	Cal	% Dif	Mea	Cal	% Dif
Water	0.994	0.990	0.4	1.010	1.006	0.4
LiF	0.986	0.981	0.5	1.004	1.002	0.2
Al ₂ O ₃	0.987	0.986	0.1	1.007	1.005	0.2

DISCUSSION

The MC model, which is based on the EGSnrc code was built, tested and validated against experimental data. The calculated photon beam distributions in a water phantom were compared to the measured distributions for field sizes ranging from $5 \times 5 \text{ cm}^2$ to $20 \times 20 \text{ cm}^2$. The fine tuning of the electron beam characteristics has been based on the depth dose curves in order to determine the energy of the electron beam. The depth dose curves showed the insensitivity of the depth dose profiles to the initial electron beam (40, 41). The percentage differences were within 2%. The results confirm and validate our simulated model.

The depth dose curves in figure 2 showed the comparison of dose distributions for the 6 and 15 MV photon beams. Immediately below the 3.5 cm silicone gel breast prosthesis at 0.5 cm depth, the doses calculated with silicone gel breast prosthesis were slightly higher than the dose calculated without the silicone gel breast prosthesis. The maximum percentage difference of 1.4% and 1.7% for 6 and 15 MV photon beams were found, respectively. The statistical uncertainty in the calculations was about 0.2%. For each radiation beam, the percentage differences were observed to decrease with increasing photon beam energy. This is due to fewer electrons set in motion in the silicone gel breast prosthesis that cause the dose degradation in the interface region. It is also believed to be due to a discontinuity in the photons producing electron fluence at this location (21).

In table 1, Dose reduction was observed for 6 MV photon beam. A maximum of 0.8% was calculated, while for 15 MV photons beam 1.2% dose enhancement was observed. For the 6 MV, the dose reduction (DEF < 1.0) was observed due to attenuation of the silicone gel breast

prosthesis. Chew *et al* (2005) established similar findings (42). This showed that fewer photons were attenuated by the prosthesis, which resulted in a decrease in the electron fluence leaving the prosthesis.

As observed in figures 3 and 4, for a given photon energy, a slight increase in DEFs with increase in silicone gel breast thicknesses was observed. This is consistent with the report in the literature (43). The change is due to the scattered photon beam contribution within an individual silicone gel breast prostheses. The 6 MV beams showed dose reduction (DEF < 1.0) while the 15 MV photon beam showed a dose enhancement (DEF > 1.0) for all the silicone gel breast prosthesis used in this study.

It can be seen from table 2 that the DEFs for the 6 and 15 MV photon beams measured with the TLDs are slightly higher than those calculated with Monte Carlo method at the same point in the interface region. The discrepancies could be attributed to the fact that this study computes the DEFs in a voxel element. DEFs calculated in a TLD sized voxels filled were within a $0.1 \times 0.1 \times 0.1 \text{ cm}^3$ voxel, which were equal to the size of the TLDs used during measurements. The measured and calculated DEF values agree well within 1.0% which confirms the validity of our simulation. It can also be seen from table 2 that the dose enhancement increases generally with increasing photon energy. The study revealed that tissue around the interface region receives enhanced dose of about 2.4% with 15 MV photon beam energy, while the 6 MV photon beam energy delivered a dose reduction of about 2.0%.

CONCLUSION

This study used the Monte Carlo simulation

to determine the DEFs caused by the silicone gel breast prosthesis in a water phantom. The findings of this work are useful for physicists and oncologists wanting to irradiate through the silicone gel breast prosthesis. We recommend that a 6 MV photon beam can be used during irradiation to minimize the dose enhancement factor at the interface region.

ACKNOWLEDGMENTS

We would like to thank the Varian Oncology System for providing useful information for Monte Carlo simulations. The Polokwane Radiation Oncology staff for assisting during measurements.

Conflicts of interest: Declared none.

REFERENCES

1. Pradhan AS, Gopala KK, Iyer PS (1992) Dose measurement at high atomic number interfaces in megavoltage photon beams using TLDs. *Med Phys*, **19**: 355-56.
2. Keall PJ, Siebers JV, Libby B, Mohan R (2003) Determining the incident electron fluence for Monte Carlo-based photon treatment planning using a standard measured data set. *Med Phys*, **30**: 574-82.
3. Webb S (1979) The absorbed dose in the vicinity of an interface between two media irradiated by a ^{60}Co source. *Br J Radiol*, **52**: 962-67.
4. Werner BL, Das IJ, Khan FM, Meigooni AS (1987) Dose perturbation at interface in photon beams. *Med Phys*, **14**: 585-95.
5. Werner BL, Das IJ, Khan FM, Meigooni AS (1990) Dose perturbation at interface in photon beams: Secondary electron transport. *Med Phys*, **17**: 212-20.
6. Das IJ, Kase KR, Meigooni AS, Khan FM, Werner BL (1990) Validity of transition-zone dosimetry at high atomic interface in megavoltage photon beams. *Med Phys*, **17**: 10-6.
7. Farahani M, Eichmiller FC, McLaughlin WL (1990) Measurement of absorbed doses near metal and dental material interfaces irradiated by gamma-ray therapy beams. *Phys Med Biol*, **35**: 369-85.
8. Das IJ (1997) Forward dose perturbation at high atomic number interfaces I kilovoltage X-rays beams. *Med Phys*, **24**: 1780-87.
9. Chatzigiannis C, Lymeropoulou G, Sandilos P, Dardoufas C, Yakoumakis E, Georgiou E, Karaiskos P (2011) Dose perturbation in the radiotherapy of breast cancer patients implanted with the Magna-site: a Monte Carlo study. *J Appl Clin Med Phys*, **12**(2): 58-70.
10. Kuske RR, Schuster R, Klein EE, Young L, Perez CA, Fineberg B (1991) Radiotherapy and breast reconstruction: Clinical results and dosimetry. *Int J Radiat Oncol Biol Phys*, **21**: 39-46.
11. Reft C, Alecu R, Das J, et al. (2003) Dosimetric considerations for patients with HIP prostheses undergoing pelvic irradiation. Report of the AAPM Radiation Therapy Committee Task Group 63. *Med Phys*, **30**: 1162-82.
12. Asena A, Kainr T, Crowe SB, Trapp JV (2015) Phantom beam dose distributions for patients with implanted temporary tissue expanders. *J Phys: Conf Ser*, **574**: 012062.
13. Damast S, Beal K, Ballangrud A, Losasso TJ, Cordeiro PG, Disa JJ, Hong L, McCormick BL (2006) Do metallic ports in tissue expanders affect postmastectomy radiation delivery? *Int J Radiat Oncol Biol Phys*, **66**: 305-10.
14. Thompson RC and Morgan AM (2005) Investigation into dosimetric effect of a MAGNA-SITE tissue expander on post-mastectomy radiotherapy. *Med Phys*, **32**(6): 1640-46.
15. Roberts R (2001) How accurate is a CT-based dose calculation on a pencil beam TPS for a patient with metallic prosthesis? *Phys Med Biol*, **46**: N227-34.
16. Medline plus Medical Encyclopaedia (2012) Mastectomy. A service of the U.S National Library of Medicine, *National Health Institutes*.
17. Shedbalkar AR, Devata DA, Padanilam T (1980) A study of effects of radiation on silicone prostheses. *Plast Reconstr Surg*, **65**: 805-10.
18. Krishnan L, St. George FJ, Mansfield CM, Krishnan EC (1983) Effect of silicone gel breast prosthesis on electron and photon dose distributions. *Med Phys*, **10**: 96-9.
19. Klein EE and Kuske RR (1993) Changes in photon dose distributions due to breast prostheses. *Int J Radiat Oncol Biol Phys*, **25**: 541-49.
20. Andreo P (1991) Monte Carlo techniques in the medical radiation physics. *Phys Med Biol*, **36**: 861-920.
21. Khan FM, Doppke KP, Hogstrom KR, et al. (1991) Clinical electron-beam dosimetry, report of AAPM Radiation Therapy Committee task Group No 25. *Med Phys*, **18**: 73-109.
22. Izewska J, Georg D, Bera P, et al. (2007) A methodology for TLD postal dosimetry audit of high-energy radiotherapy photon beams in non-reference condition. *Radiother Oncol*, **84**: 67-74.
23. Saeed AB, Muhammed AR, Aalia N (2009) An analysis of depth dose characteristic of photon in water. *J Ayub Med Coll Abbottabad*, **21**: 41-5.
24. Kawrakow I (2000) Accurate condensed history Monte Carlo simulations of electron transport, I. EGSnrc, the new EGS4 version. *Med Phys*, **29**: 485-98.
25. Kawrakow I and Rogers DWO (2007) The EGSnrc code system: Monte Carlo simulation of electron and photon transport. Technical report PIRS-701 NRC, Canada, Ottawa, 1-7.
26. Mora GM, Maio A, Rogers DWO (1999) Monte Carlo simulation of a typical ^{60}Co therapy source. *Med Phys*, **26**: 2494-505.

27. Rogers DWO, Walters B, Kawrakow I (2005) BEAMnrc user manual. NRC report PIRS 509(a) revL.
28. Rogers DWO, Walters B, Kawrakow I (2009) Beamnrc user manual. NRC report PIRS-059(a) revL.
29. Walters BRB, Kawrakow I, Rogers DWO (2005) DOSXYZnrc user manual. NRC report PIRS 794 revB.
30. Varian Oncology System Palo Alto (1996) CA Monte Carlo project, Confidential Report.
31. Rogers DWO, Walters B, Kawrakow I (2005) BEAMnrc user manual. NRC report PIRS 509(a) revL.
32. Klein EE and Kuske RR (1993) Changes in photon dose distributions due to breast prostheses. *Int J Radiat Oncol Biol Phys*, **25**: 541-49.
33. Movers MF, Mah D, Boyer SP, Chang C, Pankuch M (2014) Use of proton beams with breast prostheses and tissue expanders. *Med Dosim*, **39**: 98-101.
34. Zhang B, Zhu J, Li Y, Chen S, Chen L, Liu X (2015) Feasibility of lateral dose profile measurements in a small field using TLDs. *Phys Med Biol*, **60**: N47-57.
35. Chen SW, Wang XT, Chen LX, Tang Q, Liu XW (2009) Monte Carlo evaluations of the absorbed dose and quality dependence of Al₂O₃ in radiotherapy photon beams. *Med Phys*, **36**: 4421-4.
36. Mobit P, Agyengi E, Sandison G (2006) Comparison of the energy-response factor of LiF and Al₂O₃ in radiotherapy beams. *Radiat Prot Dosim*, **119**: 497-9.
37. Mobit PN, Mayles P, Nahum AE (1996) The quality dependence of LiF TLD in megavoltage photon beams: Monte Carlo simulation and experiments. *Phys Med Biol*, **41**: 387-98.
38. Krishnan L, St. George FJ, Mansfield CM, Krishnan EC (1983) Effect of silicone gel breast prosthesis on electron and photon dose distributions. *Med Phys*, **10**: 96-9.
39. Hrbacek J, Depuydt T, Nulens A, Swinnen A, Van den Heuvel F (2007) Quantitative evaluation of a beam-matching procedure using one-dimensional gamma analysis. *Med Phys*, **34**: 2917-27.
40. Libby B, Siebers J, Mohan R (1999) Validation of Monte Carlo generated phase space descriptions of medical linear accelerators, *Med Phys*, **26**: 1476-83.
41. Tzedakis A, Damilakis J, Mazonakis M, Stratakis J, Varveris H, Gourtsoyiannis N (2004) Influence of initial electron beam parameters on Monte Carlo calculated absorbed dose distributions for radiotherapy photon beams, *Med Phys*, **31**: 907-13.
42. Cheng CW, Mitra R, Li XA, Das IJ (2005) Dose perturbations due to contrast medium and air in MammoSite treatment: An experimental and Monte Carlo study. *Med Phys*, **32**: 2279-87.
43. Robar JL, Riccio SA, Martin MA (2002) Tumour dose enhancement using modified megavoltage photon beams and contrast media. *Phys Med Biol*, **47**: 2433-49.